

A Modified Critical Damage Model to Predict Fatigue Crack Growth under Variable Amplitude Loading Based on Low Cycle Fatigue Data

Jorge Rodríguez Durán

Volta Redonda School of Industrial and Metallurgical Engineering
Universidade Federal Fluminense (UFF), Brazil
email: duran@metal.eimvr.uff.br

Marco Antonio Meggiolaro

Jaime Tupiassú Pinho de Castro

Mechanical Engineering Department
Pontifical Catholic University of Rio de Janeiro (PUC-Rio), Brazil
e-mails: meggi@mec.puc-rio.br, jtcastro@mec.puc-rio.br

Copyright © 2004 Society of Automotive Engineers, Inc

ABSTRACT

The ϵN method can be combined with fracture mechanics concepts to *predict* fatigue crack growth behavior, assuming that the crack propagation is caused by the damage accumulated by the cyclic elastic-plastic deformations ahead of the crack tip. This model recognizes that the cyclic strain range at any given point cut by the crack path increases as the crack tip approaches its volume element, and postulate that this element failure when the crack tip reaches it is due to the accumulation of a critical damage value. According to this idea, the crack growth rate under constant ΔK loading is assumed caused by the sequential failure of identical volume elements ahead of the crack tip, whose fixed width can be calculated using the strain distribution around the crack and the ϵN methodology. In this work, this critical damage approach is extended to the variable amplitude (VA) loading case, *considering load interaction effects*. Under VA conditions, the crack increment at each load cycle is clearly not a constant, and is instead assumed equal to the region ahead of the crack tip that accumulated damage beyond some specified critical value. However, the infinity strains predicted by the usual (singular) modeling at the crack tip would invalidate any attempts to correlate ϵN and da/dN parameters. To remove this singularity, the crack is modeled as a sharp notch with a very small but finite radius, estimated to be of the CTOD order. The geometric stress concentration factor K_t of this notch is estimated using Creager and Paris method, and the now finite strains at its root are calculated using a concentration rule such as Neuber or Glinka. The strain distribution ahead of the crack tip is modeled using a modified HRR field, which is then displaced to match the calculated strain at the crack

tip. Finally the hysteresis loops and the corresponding damage at each volume element ahead of the crack tip are calculated at each event of the VA loading. The proposed approach is validated through experiments on API-5L-X52 and 1020 steel CT specimens.

Keywords: Critical damage model; Crack growth prediction; Low cycle fatigue; Variable amplitude loading

INTRODUCTION

Several theoretical models have been proposed to predict the fatigue crack growth (FCG) process using solid mechanics-based theoretical tools and basic or fundamental mechanical properties. Probably the most successful ones correlate the stress intensity range (ΔK) controlled FCG with the strain range ($\Delta \epsilon$) controlled fatigue crack initiation process. These models consider that the plastic zone r_Y ahead of the crack tip is composed by a sequence of very small volume elements, each one submitted to a different strain range, which are being broken sequentially as the crack propagates, see Fig. 1. Therefore, each of these volume elements will be submitted to elastic-plastic hysteresis loops of increasing amplitude as the crack tip approaches it. Any given volume element suffers damage in each load cycle, caused by the amplitude of the loop acting in that cycle, which in turn depends on the distance r between the volume element and the fatigue crack tip. Fracturing of the volume element at the crack tip (which cause the growth of the crack by fatigue) occurs when its accumulated damage reaches a critical value. This critical value will logically be due to the sum of the damage suffered in each load cycle, and a damage accumulation rule is required to quantify it. The linear damage or any

other accumulation rule may be used to reach this objective.

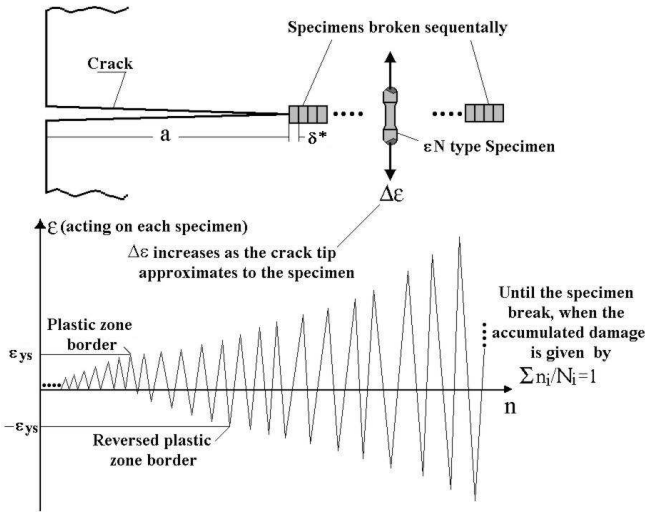


Figure 1. Fatigue crack growth caused by sequentially breaking ϵN specimens at every load cycle.

Most of the proposed critical damage models consider the width of the volume element in the crack propagation direction as being the distance that the fatigue crack propagates on each cycle [1, 2]. Others consider the fatigue crack propagation rate as being the element width divided by the number of cycles that the crack would need to cross it [3]. The theoretical models based on the low-cycle fatigue (LCF) process predict Paris' constants using the different cyclic properties of the material, and can only work in stage II of the fatigue crack propagation curve, without taking into account other factors that may influence it. However, all three stages of the da/dN curve can be modeled by modifying Paris' equation using semi-empirical relations such as McEvily's or Schwalbe's equations [4].

However, most models in the literature do not properly deal with the stress field singularity at the crack tip. As each volume element breaks when the crack tip reaches it, assuming a singular stress field implies that all damage but the one caused by this very last event would be negligible. And this same problem occurs when the elastic-plastic conditions inside the plastic zone ahead of the crack tip are considered, since the HRR strain field is also singular. It should be emphasized that this singularity is a characteristic of the models that postulate a zero radius for the crack tip, not of the real cracks which have a blunt tip when loaded. It has been proposed to simply stop the calculations before the very last loading cycle, partially solving the singularity problem but still not properly modeling the actual elastic-plastic stresses and strains at

the crack tip, which must be finite (or else the crack would be unstable).

Improved models have been proposed to calculate the actual strain ϵ^* at the crack tip from strain concentration rules [5]. In these models, the geometric stress concentration factor is estimated from the Creager and Paris [6] solution for a blunt crack tip. The HRR strain solution is then upper-bounded by the calculated crack-tip strain ϵ^* , which is assumed to be constant over the entire Region I in Figure 2, where the singular HRR solution would predict strains greater than ϵ^* .

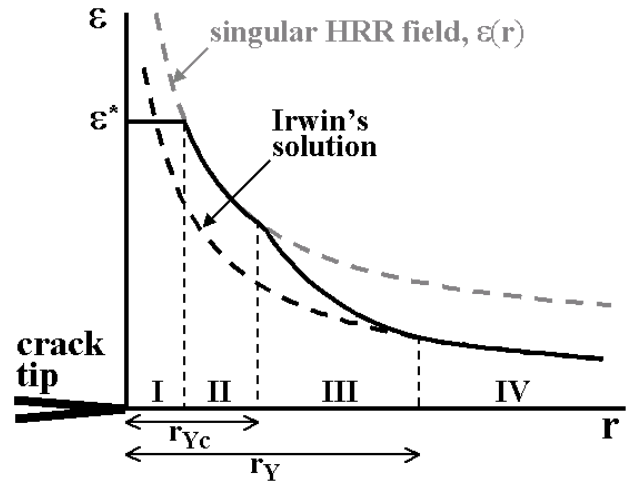


Figure 2. Theoretical strain distribution ahead of the crack tip (solid line).

This approximation, however, does not account for the stress redistribution due to the somehow arbitrarily imposed upper bound. Assuming that fatigue damage is restricted to this Region I, the number of cycles N^* associated with the constant strain range $\Delta\epsilon^*$ is obtained from Coffin-Manson. The crack growth rate da/dN is then estimated as the length of Region I divided by N^* . Such models cannot be physically justified for two reasons, as follows. First, neglecting the fatigue damage in Regions II through IV in Figure 2 is highly non-conservative, implying that the entire damage would be concentrated in these few N^* cycles. And second, such mathematical model assumes intermittent crack growth (grouped by N^* cycles instead of cycle-by-cycle) which, although valid in some cases of crazing in polymers, is certainly not the case for the great majority of metallic structures, as verified by microscopic observations of fatigue striations.

Recently, an improved model that try to simulate the actual non-singular elastic-plastic strain field around the crack tip has been proposed [7-8]. This model uses ϵN parameters and expressions of the HRR type to represent the elastic-plastic strain range inside the plastic zone ahead

of the crack tip. In this formulation, the crack tip is modeled as a sharp notch with a very small but finite tip radius to remove its singularity. Inspired by the Creager and Paris K_t solution, the origin of the HRR field is shifted from the crack tip to a point inside the crack, located by matching the (now finite) HRR strain at the crack tip with the strain predicted at that point by a strain concentration rule, such as Neuber, Glinka, or the linear rule [3]. A very reasonable agreement between the predictions and the experiments has been obtained for three structural materials - SAE1020 and API 5L X-60 steels, and 7075 T6 Al alloy - using the calculated crack growth constant in McEvily rule to predict the da/dN vs. ΔK curve [4, 7-8].

The idea that the FCG is caused by the sequential failure of volume elements ahead of the crack tip is extended here to deal with the variable amplitude loading case, which has idiosyncrasies that must be treated appropriately. First, the volume elements must have variable width, which should be calculated at every load cycle by locating the point ahead of the crack tip where the accumulated damage reaches an specified value, e.g. 1.0 when using Miner's rule, assuming that the damage is caused solely by the cyclic plastic deformations induced by the loading. In this case, the load sequence effects, such as overload-induced crack growth retardation, are associated only to the (weak) mean load effect on the ϵN curve. However, an Elber-type opening load concept can be introduced into the model, to separate the cyclic damage from the closure contributions (which are both plasticity-induced) to the crack growth process. Experiments with variable amplitude load histories are used to validate the proposed models, using the powerful numerical tools available in the ViDa software [9].

CONSTANT AMPLITUDE LOADING

The proposed model assumes that FCG is caused by the sequential fracturing of small volume elements ahead of the crack tip. In every load cycle, each one of these volume elements is submitted to elastic-plastic hysteresis loops of increasing amplitude as the crack tip approaches it, suffering a damage increment that is a function of the loop amplitude in that cycle, which depends on the distance r between the volume element and the fatigue crack tip. The fracture of the volume element at the crack tip, which is the event that causes the fatigue crack propagation, occurs when its accumulated damage reaches a critical value, quantified by some damage accumulation rule, e.g., Miner's rule:

$$\sum \frac{n_i}{N_i} = 1 \quad (1)$$

where n_i is the number of cycles of the i -th load event and N_i is the number of cycles that the piece would last if loaded solely by that event.

Under constant ΔK loading, in every load cycle the crack advances a fixed distance da . Thus, neglecting the damage accumulated outside the cyclic plastic zone r_{Yc} , there are r_{Yc}/da elements ahead of the crack tip at any instant. Since the plastic zone advances with the crack, each new load cycle breaks the element adjacent to the crack tip, induces an increased loop amplitude in all other unbroken elements (because the crack tip approaches all of them by da), and adds a new element to the damage zone. Therefore, the number of load cycles per growth increment is $n_i = 1$ and, since the elements are considered as small ϵN specimens, they break when:

$$\sum_{i=0}^{r_{Yc}/da} \frac{1}{N(r_{Yc} - i \cdot da)} = \sum_{r_i=0}^{r_{Yc}} \frac{1}{N(r_i)} = 1 \quad (2)$$

where $N(r_i) = N(r_{Yc} - i \cdot da)$ is the fatigue life corresponding to the strain range $\Delta\epsilon(r_i)$ acting at r_i from the crack tip. If ϵ_f' is the coefficient and c is the exponent of the plastic part of Coffin-Manson's rule, and assuming a perfect coherence between Coffin-Manson's and Ramberg-Osgood's elastic and plastic terms, then

$$N(r_i) = \frac{1}{2} \left(\frac{\Delta\epsilon_p(r_i)}{2\epsilon_f'} \right)^{1/c} \quad (3)$$

where $\Delta\epsilon_p(r_i)$ is the plastic strain range at r_i .

The plastic strain range inside the cyclic plastic zone can be described by Schwalbe's [4] modification of the HRR field [10, 11]:

$$\Delta\epsilon_p(r_i) = \frac{2S_{Yc}}{E} \cdot \left(\frac{r_{Yc}}{r_i} \right)^{\frac{1}{1+n'}} \quad (4)$$

where n' is the Ramberg-Osgood cyclic strain hardening exponent and S_{Yc} is the cyclic yield strength. Note that the cyclic plastic zone size in plane strain r_{Yc} is given by [12]:

$$r_{Yc} = \frac{(1-2\nu)^2}{4\pi \cdot (1+n')} \cdot \left(\frac{\Delta K}{S_{Yc}} \right)^2 \quad (5)$$

In addition, if Morrow's elastic-plastic ϵN equation is considered above instead of Coffin-Manson's rule, then mean load σ_m effects can also be accounted for. Substituting Equation (4) in Equation (3) results in

$$N(r_i) = \frac{1}{2} \left[\frac{S_{Yc}}{E \epsilon'_f} \cdot \left(\frac{r_{Yc}}{r_i} \right)^{\frac{1}{1+n'}} \right]^{1/c} \quad (6)$$

Considering the width of volume elements da as a differential distance dr ahead of the crack tip, and approximating the Miner's summation by an integral, which is easier to deal with in the calculations:

$$\frac{da}{dN} = \int_0^{r_{Yc}} \frac{dr}{N(r)} \quad (7)$$

The HRR field used to describe the stress and strain fields inside the plastic zone ahead of the idealized crack tip is singular for $r = 0$. Thus, $N(r) \rightarrow 0$ when $r \rightarrow 0$, what is not physically reasonable. However, no real crack has a zero radius tip, nor its strain field can be singular, since an infinite strain is physically impossible. This of course does not mean that singular *models* are useless. They can make powerful predictions, but among them is *not* the damage at the crack tip. However, it is easy to eliminate the strain singularity by shifting the HRR coordinate system origin into the crack by a small distance X , following Creager's idea [6]. In this case, Equation (4) becomes

$$\Delta \epsilon_p(r+X) = \frac{2S_{Yc}}{E} \cdot \left(\frac{r_{Yc}}{r+X} \right)^{\frac{1}{1+n'}} \quad (8)$$

Equations (3) and (8) are then applied to Equation (7), resulting in

$$\frac{da}{dN} = \int_0^{r_{Yc}} \frac{dr}{N(r+X)} \quad (9)$$

To determine X and $N(r+X)$ two paths can be followed. The first considers, as Creager and Paris [6] did, $X = \rho/2$, ρ being the actual crack tip radius, which can be estimated by $\rho = CTOD/2$. An expression for the CTOD of a strain hardening material can be obtained in the cyclic plastic zone using the elastic solution for displacements in Mode I [13] and the expression for r_{Yc} . As $\rho = CTOD/2$, the parameter $X = \rho/2$ to displace the functions in this group of models can be defined by

$$X = \frac{\rho}{2} = \frac{CTOD}{4} = \frac{K_{max}^2 \cdot (1-2\nu)}{\pi \cdot E \cdot S_{Yc}} \cdot \sqrt{\frac{1}{2(1+n')}} \quad (10)$$

The second path is more reasonable. Instead of arbitrate the strain field origin offset, it determines X by first calculating the plastic strain range $\Delta \epsilon_p(X)$ acting at the blunt crack tip (which is being modeled as a notch,

with a sharp but not zero tip radius), using a strain concentration rule and the crack linear elastic stress concentration factor K_t . This path also uses Creager and Paris idea [6], who solved the deep notch K_t problem under linear elastic conditions using the $\rho/2$ coordinate origin displacement, but this time only to obtain

$$K_t \cdot \Delta \sigma_n = \frac{2\Delta K}{\sqrt{\pi \rho}} \quad (11)$$

For any given ΔK and R combination it is possible to calculate ρ using Equation (10) and to obtain the product $K_t \cdot \Delta \sigma_n$ from the above equation. Then, using a strain concentration rule, the plastic strain range $\Delta \epsilon_p$ at the crack tip (where $r = 0$) is calculated. These strain concentration rules allow the determination of the plastic stress and strain ranges in a notch root if the elastic stress concentration factor K_t is known. The solution depends on the material stress-strain law, which here is assumed parabolic with a strain hardening exponent n' and with a negligible elastic range.

The strain concentration rules considered in this work are the Linear, Neuber and Glinka's rules. The Linear rule is the simplest, resulting in a plastic strain range at the crack tip given by

$$\Delta \epsilon_p = \frac{K_t \cdot \Delta \sigma_n}{E} = \frac{2\Delta K}{E \sqrt{\pi \cdot CTOD/2}} \quad (12)$$

Neuber's rule requires solving the following equations for both crack tip stress and strain ranges $\Delta \sigma$ and $\Delta \epsilon_p$

$$\Delta \sigma \cdot \Delta \epsilon_p = \frac{(K_t \Delta \sigma_n)^2}{E} = \frac{8\Delta K^2}{E \cdot \pi \cdot CTOD} \quad (13)$$

$$\Delta \epsilon_p = 2 \left(\frac{\Delta \sigma}{2H'} \right)^{1/n'}$$

Another strain concentration rule is Glinka's, where the plastic strain range $\Delta \epsilon_p$ at the crack tip is calculated from

$$\frac{2\Delta K^2}{E \cdot \pi \cdot CTOD} = \frac{\Delta \sigma^2}{4E} + \frac{\Delta \sigma}{1+n'} \cdot \left(\frac{\Delta \sigma}{2H'} \right)^{1/n'} \quad (14)$$

$$\Delta \epsilon_p = 2 \left(\frac{\Delta \sigma}{2H'} \right)^{1/n'}$$

After calculating $\Delta \epsilon_p$ at the crack tip from one of the above rules, the value of X is obtained from Equation (8) using $r = 0$, resulting in

$$\Delta\varepsilon_p = \frac{2S_{Yc}}{E} \cdot \left(\frac{r_{Yc}}{X}\right)^{\frac{1}{1+n'}} \Rightarrow$$

$$X = r_{Yc} \cdot \left(\frac{2S_{Yc}}{E\Delta\varepsilon_p}\right)^{1+n'} \quad (15)$$

The strain distribution at a distance r ahead of the crack tip, $\Delta\varepsilon_p(r+X)$, now without the singularity problem at the crack tip, is then readily obtained from Equations (8) and (15). The fatigue crack propagation rate is then calculated from Equation (9) as:

$$\frac{da}{dN} = \int_0^{r_{Yc}} 2 \cdot \left(\frac{2\varepsilon'_f}{\Delta\varepsilon_p(r+X)}\right)^{1/c} dr \quad (16)$$

Note that due to the non-linearity of Coffin-Manson's εN curve, the damage at the volume elements beyond the current cyclic yield zone (or, more conservatively, beyond the monotonic yield zone) were neglected in the above integral, simplifying the numerical calculations.

VARIABLE AMPLITUDE LOADING

Under variable amplitude loading, the FCG rate *cannot* be assumed constant because ΔK can vary at each load cycle. The models developed above can be indirectly used to calculate FCG under VA loading by integrating the predicted (under constant ΔK) da/dN curve using the cycle by cycle method. However, the idea here is to *directly* quantify the fatigue damage induced by the VA loading considering the crack growth as the result of the sequential fracturing of small variable size volume elements inside the cyclic plastic zone ahead of the crack tip.

Since the model based on the Linear strain concentration rule resulted in the best predictions in [7] (because the fatigue crack propagation data were obtained under dominant plane strain conditions), it is the only one used below. And since load interaction effects can have a significant importance in FCG, they can also be introduced in the model, e.g., considering mean load σ_m effects by:

$$N(r+X) = \frac{1}{2} \left(\frac{\Delta\varepsilon_p(r+X)}{2\varepsilon'_f} \left(1 - \frac{\sigma_m}{\sigma'_f} \right)^{-c/b} \right)^{1/c} \quad (17)$$

where σ'_f is the coefficient and b is the exponent of the elastic part of the Morrow elastic-plastic εN rule. And to separate the damage and the closure contributions to FCG (considering crack closure as the only crack retardation mechanism), an Elber-type opening load concept can be easily implemented for $R > 0$ to filter the loading cycles that cause no damage by using:

$$\Delta K_{\text{eff}} = \frac{\Delta K - \Delta K_{\text{th}}}{1-R} \quad (18)$$

The damage function for each cycle is then obtained as a function of r :

$$d_i(r+X_i) = \frac{n_i}{N_i(r+X_i)} \quad (19)$$

If the piece is virgin, then the crack increment δa_1 caused by the first load event is the value $r = r_1$ that makes Equation (19) equal to one

$$d_1(r_1+X_1) = 1 \Rightarrow \delta a_1 = r_1 \quad (20)$$

In all subsequent events, the crack increments take into account the damage accumulated by the previous loading, in the same way it was done for the constant loading case. But as the coordinate system moves with the crack, a coordinate transformation of preceding damage functions is necessary:

$$D_i = \sum_{j=1}^i d_j \left(r + \sum_{p=j}^{i-1} \delta a_p \right) \quad (21)$$

Since the distance $r = r_i$ where the accumulated damage equals one in the i -th event is a variable that depends on ΔK_i (or $\Delta K_{\text{eff}i}$) and on the previous loading history, elements of different widths may be broken by this model.

RESULTS AND DISCUSSION

FCG experiments under variable amplitude loading were performed using API-5L-X52 steel CT specimens, 50 mm wide by 10 mm thick. Pre-cracking was made under constant amplitude loading with $\Delta K = 20 \text{ MPa}/\text{m}^{1/2}$ until reaching $a = 12.55 \text{ mm}$ ($a/w = 0.25$). FCG occurred under LEFM conditions. Testing was conducted in a 100 kN computer-controlled servo-hydraulic machine. Crack size was monitored within a $20\mu\text{m}$ accuracy by the Back Face Strain technique [14], using a 5mm 120Ω strain gage.

Oligocyclic fatigue tests were carried out under axial strain control according to the ASTM E 606-92 specifications [15], using the same equipment described above. Two specimens were tested at each strain amplitude, and to obtain the εN curve fifty specimens were tested under deformation ratios varying from $R = -1$ to $R = 0.8$, see Figure 3. The test frequency varied between 1 and 10 Hz, and the data acquisition system sampled a minimum of 500 points per cycle. The module method (ASTM E 606-92) was used to determine the fatigue life. The measured material properties are shown in the table below.

Table 1. Mechanical properties of the API 5L X52 steel.

E [GPa]	200
S_u [MPa]	527
S_y [MPa]	430
S_y' [MPa]	370
H' [MPa]	840
n'	0.132
σ'_f [MPa]	720
ϵ'_f	0.31
b	-0.076
c	-0.53
ΔK_{th} (R=0.1) [MPa \sqrt{m}]	8.0
da/dN (R=0.1) [m/cycle]	$2 \cdot 10^{-10} \cdot (\Delta K - 8)^{2.4}$

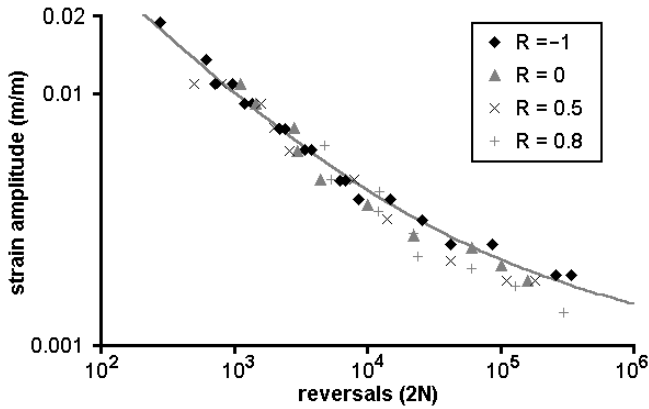


Figure 3. Measured and fitted strain-life data for the API 5L X52 steel.

Note from Figure 3 that this steel is almost insensitive to the deformation R ratio, in special for short lives. Note also that this data does include very high R tests. Morrow's strain-life equation, which includes the mean stress effect only in Coffin-Manson's elastic term, was found to best fit the experimental data. Morrow's fitted equation is plotted for $R = -1$ in Figure 3.

Crack growth was then conducted at 25 Hz under a VA load history consisting of a series of 50,000 blocks containing 100 reversals (50 cycles) each, as shown in Figure 4. The high mean stress levels were chosen to avoid crack closure effects, since they were not yet included in the model at the testing time (even though they can be easily accounted for when drawing the hysteresis loops). The load history was counted by the sequential rain-flow method [16]. The damage calculation was made using a specially developed code and the linear strain concentration rule. Figure 5 compares the predictions and experiments.

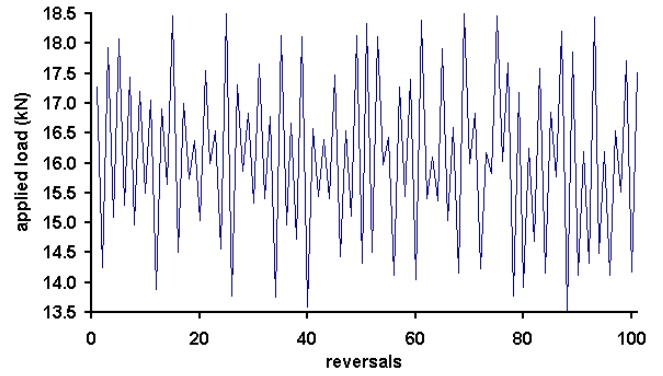


Figure 4. Load block applied to the API 5L X52 steel CTS.

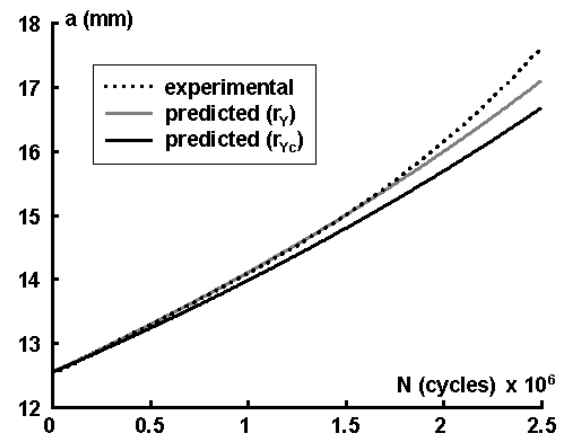


Figure 5. Comparison between crack growth measurements and eN-based predictions (API 5L X52 steel).

As seen in Figure 5, the crack growth predictions under variable amplitude loading based solely on eN parameters were quite accurate. The prediction that assumed no damage outside the cyclic plastic zone r_{v_c} (solid black line in Figure 5) underestimated crack growth. However, when the small (but significant) damage in the material between the cyclic and monotonic plastic zone borders is also included in the calculations, then an even better agreement is obtained (gray line in Figure 5). Note also that crack growth is slightly underestimated after $1.8 \cdot 10^6$ cycles, probably due to having neglected the elastic damage and the mean stress effects.

Similar tests were conducted using AISI 1020 steel CT specimens of the same dimensions described above. The measured material properties are shown in the table below.

Table 2. Mechanical properties of the AISI 1020 steel.

E [GPa]	205
S_u [MPa]	491
S_y [MPa]	285

S_v' [MPa]	270
H' [MPa]	941
n'	0.18
σ'_f [MPa]	815
ϵ'_f	0.25
b	-0.114
c	-0.54
ΔK_{th} (R=0.1) [MPa \sqrt{m}]	11.6
da/dN (R=0.1) [m/cycle]	$5 \times 10^{-10} (\Delta K - \Delta K_{th})^2 \cdot \left[\frac{277}{277 - \Delta K / (1 - R)} \right]$

The VA load history was a series of blocks containing 101 peaks and valleys, as shown in Figure 6, with a duration of two seconds each. Figure 7 compares the predictions with the experimentally obtained data.

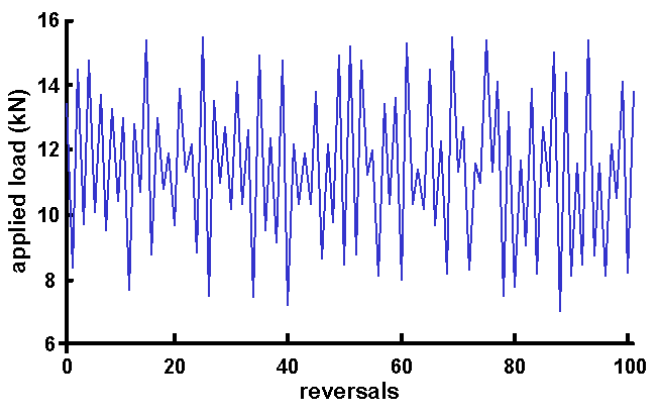


Figure 6. Load block applied to the AISI 1020 steel CTS.

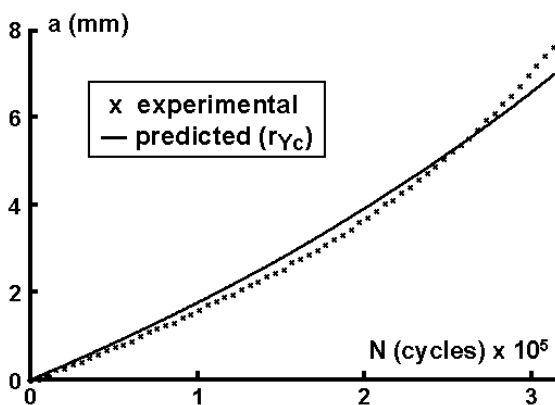


Figure 7. Comparison between crack growth measurements and ϵN -based predictions (AISI 1020 steel).

This other prediction of fatigue crack growth under VA based only on ϵN properties turn out to be again quite accurate. This indicates that the ideas behind the critical damage model discussed above make sense and deserve be better explored.

ACKNOWLEDGEMENTS

The authors would like to thank eng. Marcelo Gomes de Souza for obtaining the experimental results presented in Table 1 and Fig. 3, and to CNPq, the Brazilian Research Council, and to CAPES, a Brazilian Education Ministry agency, for their support.

CONCLUSIONS

A damage accumulation model, entirely based on ϵN cyclic properties, was proposed for predicting fatigue crack propagation under variable amplitude loading. The stress field singularity is removed by modeling the crack as a sharp notch with a small but finite radius equal to half the CTOD. The HRR field is then modified using some strain concentration rule, such as Neuber, Glinka, or the linear rule, and damage accumulation is explicitly calculated at each load cycle. Due to the non-linearity of Coffin-Manson's ϵN curve, the damage at the volume elements beyond the current yield zone may be neglected, simplifying the numerical calculations. Experimental results on API 5L X52 steel and 1020 steel show a good agreement between measured crack growth under VA loading and the predictions based purely on ϵN data. This methodology can be complemented by strip-yield model calculations, which are used to predict the crack closure caused by the residual strains at the crack faces. Moreover, the effect of residual stress fields ahead of the crack tip can be directly accounted for when drawing the hysteresis loops, providing a powerful physical model to understand crack retardation effects based solely on ϵN concepts.

REFERENCES

- [1] Majumdar S, Morrow J. Correlation Between Fatigue Crack Propagation and Low Cycle Fatigue Properties. In: Fracture Toughness and Slow-Stable Cracking, ASTM STP 559, 1974. pp. 159-182.
- [2] Castro JTP, Kenedi PP. Previsão das Taxas de Propagação de Trincas de Fadiga Partindo dos Conceitos de Coffin-Manson. Journal of the Brazilian Society of Mechanical Sciences, 1995;17(3):292-303.
- [3] Glinka G. A Notch Stress-Strain Analysis Approach to Fatigue Crack Growth. Eng. Fracture Mechanics, 1985; 21(2):245-61.

- [4] Schwalbe KH. Comparison of Several Fatigue Crack Propagation Laws with Experimental Results. Eng. Fracture Mechanics, 1974;6(2-H):325-41.
- [5] Glinka G. A Cumulative Model of Fatigue Crack Growth. Int. J. Fatigue, 1982;4:59-67.
- [6] Creager M, Paris PC. Elastic Field Equations for Blunt Cracks with Reference to Stress Corrosion Cracking. Int. J. of Fracture Mechanics, 1967;3:247-52.
- [7] Durán JAR, Castro JTP, Payão Filho JC. Fatigue Crack Propagation Prediction by Cyclic Plasticity Damage Accumulation Models. Fatigue and Fracture of Eng. Materials and Structures, 2003;26(2):137-50.
- [8] Durán JAR, Castro JTP, Meggiolaro MA. A Damage Accumulation Model to Predict Fatigue Crack Growth under Variable Amplitude Loading Using ϵ_N Parameters. Fatigue 2002, Emas, 2002:2759-76.
- [9] Meggiolaro MA, Castro JTP. ViDa - a Visual Damagemeter to Automate the Fatigue Design under Complex Loading (in Portuguese). Brazilian Journal of Mechanical Sciences - RBCM 1998;20(4):666-85.
- [10] Hutchinson JW. Singular Behavior at the End of a Tensile Crack in a Hardening Material. J. of the Mechanics and Physics of Solids, 1968;16(1):13-31.
- [11] Rice JR, Rosengren GF. Plane Strain Deformation Near a Crack Tip in a Power Law Hardening Material. Journal of the Mechanics and Physics of Solids, 1968;16(1):1-12.
- [12] Schwalbe, KH. Approximate Calculation of Fatigue Crack Growth. Eng. Fracture Mech., 1973;9(4):381-95.
- [13] Latzko, DGH. Linear Elastic Fracture Mechanics: A summary review. In Post-Yield Fracture Mechanics, ch. 1, Applied Science Publishers Ltd., London, 1979.
- [14] Shaw WJD, Zhao W. Back Face Strain Calibration for Crack Length Measurements. Journal of Testing and Evaluation, 1994;22(6):512-16.
- [15] ASTM Standard E606-92, Standard Practice for Strain-Controlled Fatigue Testing. Annual Book of ASTM Standards, vol. 03.01. American Society for Testing and Materials, West Conshohocken, PA. 1997:523-37.
- [16] Miranda ACO, Meggiolaro MA, Castro JTP, Martha LF, Bittencourt TN. Fatigue Crack Propagation under Complex Loading in Arbitrary 2D Geometries. In: Braun AA, McKeighan PC, Lohr RD, editors. Applications of Automation Technology in Fatigue and Fracture Testing and Analysis, vol. 4. ASTM STP 1411, 2002:120-46.